

Circulating CCRR serves as potential novel biomarker for predicting acute myocardial infarction

Lina Xuan^{1#}, Huishan Luo^{1#}, Shu Wang^{2#}, Guangze Wang¹, Xingmei Yang¹, Jun Chen¹, Jianjun Guo¹, Xiaomeng Duan¹, Xiufang Li¹, Hua Yang¹, Shengjie Wang¹, Hailong Zhang¹, Qingqing Zhang¹, Shulei Liu², Yongtao She², Kai Kang^{3,4*}, Lihua Sun^{1,3*}

Abstract

Objective: Cold regions exhibit a high prevalence of cardiovascular disease, particularly acute myocardial infarction (AMI), which is one of the leading causes of death associated with cardiovascular conditions. Cardiovascular disease is closely linked to the abnormal expression of long non-coding RNA (lncRNA). This study investigates whether circulating levels of lncRNA cardiac conduction regulatory RNA (CCRR) could serve as a biomarker for AMI. **Materials and methods:** We measured circulating CCRR from whole blood samples collected from 68 AMI patients and 69 non-AMI subjects. An AMI model was established using C57BL/6 mice. Quantitative reverse transcription PCR (qRT-PCR) was used to assess CCRR expression. Exosomes were isolated from cardiomyocytes, and their characteristics were evaluated using electron microscope and nanoparticle tracking analysis. The exosome inhibitor GW4869 was employed to examine the effect of exosomal CCRR on cardiac function using echocardiography. Protein expression was detected using Western blot and immunofluorescence staining. **Results:** The circulating level of CCRR was significantly higher in AMI patients (1.93 ± 0.13) than in non-AMI subjects (1.00 ± 0.05 , $P < 0.001$). The area under the ROC curve (AUC) of circulating CCRR was 0.821. Similar changes in circulating CCRR levels were consistently observed in an AMI mouse model. Exosomal CCRR derived from hypoxia-induced cardiomyocytes and cardiac tissue after AMI were increased, a change that was reversed by GW4869. Additionally, CCRR-overexpressing exosomes improved cardiac function in AMI. **Conclusion:** Circulating lncRNA CCRR is a potential predictor of AMI. Exosomal CCRR plays a role in the communication between the heart and other organs through circulation.

Keywords

acute myocardial infarction; lncRNA; cardiac conduction regulatory RNA; exosome

Received 01 April 2024, accepted 07 June 2024

¹Department of Pharmacology, Harbin Medical University (the State-Province Key Laboratories of Biomedicine-Pharmaceutics of China, Key Laboratory of Cardiovascular Research, Ministry of Education, Joint International Research Laboratory of Cardiovascular Medicine Research, Ministry of Education), College of Pharmacy, State Key Laboratory of Frigid Zone Cardiovascular Diseases (SKLFZCD), Harbin Medical University, Harbin 150000, China

²Department of Cardiology, the First Affiliated Hospital, Harbin Medical University, Harbin 150000, China

³Department of Cardiovascular Surgery, the First Affiliated Hospital of Harbin Medical University, Harbin 150000, China

⁴NHC Key Laboratory of Cell Transplantation, the First Affiliated Hospital of Harbin Medical University, Harbin 150000, China

*Corresponding authors Lihua Sun, E-mail: sunlihua0219@163.com; Kai Kang, E-mail: kangkai1975@sina.com

[#]These authors contributed equally to this work.

Open Access. © 2024 The author (s), published by De Gruyter on behalf of Heilongjiang Health Development Research Center. This work is licensed under the Creative Commons Attribution 4.0 International License.

1 Introduction

The incidence of acute myocardial infarction (AMI) is currently on the rise, contributing significantly to high mortality and morbidity worldwide. In 2019, there were approximately 523 million cases and 18.6 million deaths globally^[1]. The Global Burden of Disease Study highlights significant geographical differences in cardiovascular disease mortality rates^[2]. An epidemiological study in Asia reveals that mortality from cardiovascular disease is higher in Central and East Asian countries compared to South and Southeast Asian countries^[3]. A cohort study on cardiovascular risk factors in China indicates that the prevalence of high cardiovascular disease risk is relatively higher in Northeast China and

North China, with the highest rates observed in Northeast China^[4]. Northeast China, being a cold region, experiences an increased risk of cardiovascular diseases due to cold-induced changes in the autonomic nervous system, blood pressure, coagulation system, inflammatory response, and oxidative stress^[5]. However, previous research on the population risk of cardiovascular disease has limitations, such as limited sample size, narrow distribution of study populations, and a restricted range of risk factors. Early detection is important for the treatment and prognosis of patients with AMI. A reliable noninvasive serum marker is needed for the early identification of AMI patients. Current markers for cardiac muscle necrosis, such as creatine kinase MB (CK-MB), cardiac troponin I (cTnI), Cardiac myosin-binding protein C (cMyBP-C)

are useful for detecting AMI^[6]. Additionally, biomarkers like soluble suppression of tumorigenicity 2 (sST2), galectin 3 (Gal-3), and bio-ADM correlate with congestion severity and identify risk of death. Growth differentiation factor 15 (GDF-15) might identify a high risk for recurrent cardiovascular events, but these markers have several limitations^[7]. Therefore, it is imperative to find more reliable biomarkers especially for the early diagnosis of AMI.

More recently, long non-coding RNAs (lncRNAs) have emerged as an important component of the gene regulatory network. lncRNAs are a class of non-coding RNAs greater than 200 nucleotides in length, lacking significant open reading frames or protein-coding capacity^[8]. These transcripts are widely distributed in the cytoplasm and nucleus and are the most abundant class of non-coding RNAs with highly complex functions^[9]. lncRNAs participate in numerous physiological and pathological processes, playing regulatory and structural roles in various biological processes^[10]. The clinical application value and pathophysiological mechanisms of circulating have been studied lncRNAs as potential biomarkers of cardiovascular diseases^[11-13]. Several lncRNAs have been detected in circulation, and we have summarized the potential of these lncRNAs as circulating biomarkers in cardiovascular diseases^[14]. Our previous study identified lncRNA-ZAFS1 and lncRNA-CDR1AS as potential diagnostic biomarkers in whole blood of patients with AMI^[15]. Early circulating CHAST expression is associated with cardiac contractile function in AMI patients^[16]. UCA1 levels in the plasma of AMI patients decrease in the early stage of the disease and increase three days after the onset of myocardial infarction (MI)^[17]. Gao *et al.* showed that HOTAIR is significantly downregulated in the early stage of AMI^[18]. MIAT is associated with MI through single nucleotide polymorphism (SNP) association experiment^[19]. NEAT1 is part of a molecular circuit involving several chemokines and interleukins that are persistently deregulated post-MI^[20]. LIPCAR expression is downregulated after MI and upregulated in late MI^[21]. NRF is a potential biomarker of heart failure after AMI^[22]. These findings suggest that lncRNAs serve as potential biomarkers for cardiovascular diseases.

Our previous study has demonstrated that CCRR is a potential antiarrhythmic target in heart failure, functioning as a signaling mechanism for increased Cx43 protein in the plasma membrane by targeting CIP85^[23]. However, the role of CCRR in MI and its potential as a diagnostic marker for MI have not been fully elucidated. Therefore, this study aims to identify the expression changes of CCRR in whole blood after AMI and evaluate its potential as a diagnostic marker for AMI. We collected whole blood samples from AMI patients and non-AMI patients to detect the expression level of CCRR. Additionally, we analyzed the predictive power of lncRNA CCRR for cardiac risk events, correlated its levels with known biomarkers, and assessed the regulatory role of lncRNA CCRR in cardiac function. Ultimately, a comprehensive

understanding of how cardiac-derived exosomes promote CCRR trafficking from the myocardium to circulating could provide a basis for novel therapeutic interventions to improve cardiac function following MI.

2 Materials and methods

2.1 Patient samples

This study was conducted in accordance with the Declaration of Helsinki and approved by the Ethnic Committee for the Use of Human Samples at Harbin Medical University. All procedures involving human participants were approved by the Institutional Research Board of Harbin Medical University (No. IRB5003621). Written informed consent was obtained from all study participants. All animal procedures were approved by the Institutional Animal Care and Use Committee at Harbin Medical University.

2.2 Animals

The Experimental Animal Center of Harbin Medical University provided male C57BL/6 mice, aged between 8 and 10 weeks and weighing between 20 and 25 grams. All mice were raised in a standard cage with a humidity of 50% ± 20%, a temperature of 23 ± 3°C, and a 12-h light/12-h dark cycle. The mice were kept in the same room with free access to food and water. All experiments complied with the guiding principles for the care and use of laboratory animals at Harbin Medical University and were approved by the Ethics Committee for Animal Experimentation of the School of Pharmacy, Harbin Medical University (No. IRB5003621, No. IRB3001823). Additionally, all animal procedures conformed to the guidelines of Directive 2010/63/EU of the European Parliament on the protection of animals used for scientific purposes.

2.3 Primary culture of cardiomyocytes from neonatal mice

Cardiomyocytes were isolated from mice aged 1 to 3 days. In brief, the isolated mouse hearts were washed and chopped in Dulbecco's modified Eagle medium (DMEM) buffer (Biological Industries, Haemek, Israel). The cardiac tissue was digested in trypsin (Beyotime, Shanghai, China) for 12 h and then terminated with DMEM containing 10% Fetal bovine serum (FBS). Subsequently, the cardiac tissue was digested by 0.8 mg/mL type II collagenase digestive solution. The resulting cell precipitate was resuspended in DMEM buffer with 10% FBS. For subsequent experiments, cardiomyocytes were collected and inoculated on culture plates for 48 h. To simulate hypoxic conditions, it is essential to maintain the pH balance and metabolic activity of the cardiomyocytes. The cardiomyocytes were cultured under hypoxia conditions at 37°C,

with 5% CO₂, 1% O₂ and 94% N₂ for 12 h. The culture medium was collected for exosomes isolation.

2.4 Collection of human blood samples

Whole blood sample from 68 AMI patients and 69 non-AMI control subjects were collected from the First Affiliated Hospital of Harbin Medical University (Harbin, China). The samples were obtained *via* direct venous puncture and collected into the blood collection tubes containing EDTA.

2.5 AMI mice model

The mice were anesthetized by intraperitoneal injection of 2,2,2-tribromoethanol (Avertin, 0.2 g/kg body weight, Sigma, St. Louis, MO, USA). The thorax was opened at the point of the most pronounced cardiac pulsation to expose the heart. The left anterior descending (LAD) coronary artery was tied with a silk thread, and the chest was subsequently closed. Before surgery, mice in the GW4869 group received an intraperitoneal injection of GW4869 (2.5 mg/kg, MCE). Sham-operated mice served as controls, undergoing the same procedure but without ligation of the LAD coronary artery. For the exosomes administration groups, CCRR-Exos or NC-Exos were injected into the mice *via* the tail vein. In parallel, sham-operated mice were injected with the same volume of PBS. Model mice with elevated S-T segment in ECGs, confirmed to be suffering from ischemia, were included in the AMI group for follow-up studies.

2.6 Exosomes isolation

Exosomes were isolated by differential centrifugation. The left ventricular tissue of mice, following AMI injury, was removed, washed in PBS, sheared, and digested for 30 min at 37°C in collagenase type II digestion solution (Gibco, USA). Residual tissue and cells were then removed by centrifugation at 1,000 g for 10 min. The supernatant was collected and centrifuged at 3,000 g for 10 min, followed by centrifugation at 10,000 g for 10 min at 4°C. The supernatant was then filtered through a 0.22 µm microporous membrane. The filtered supernatant was centrifuged at 100,000 g for 2 h at 4 °C to pellet all exosomes (Optima L-100XP Ultra centrifuge, Beckman Coulter). After washing with PBS, the exosomes were resuspended in 200 µL PBS for subsequent experiments.

2.7 Electron microscope

The freshly isolated cardiomyocyte exosome suspensions were loaded onto 200-mesh carbon-coated Formvar grids for 5 min, and then stained with 2% phosphotungstic acid for 5 min at room temperature. The exosome samples were examined using a

transmission electron microscope (TEM; Hitachi, HT7700).

2.8 Nanoparticle tracking analysis (NTA)

The particle size distribution of the exosomes was analyzed using nanoparticle tracking analysis (NTA) by the NanoFCM N30E.

2.9 Exosomes label and uptake experiments

In the exosome uptake experiment, we used the PKH26 Red Fluorescent Cell Linker Mini Kit (Sigma-Aldrich, USA) to label the exosomes. The isolated exosomes were resuspended in PBS, and 100 µL of the exosome suspension was added to 200 µL diluent C. The PKH26 dye was mixed with Diluent C for 5 min at room temperature. The reaction was terminated with 5% BSA in PBS. The labeled exosomes were then isolated using the Ribo™ Exosome Isolation Reagent (Ribobio, China) and resuspended in 100 µL PBS for the uptake experiment. Primary neonatal mouse cardiomyocytes were labeled with α-actinin (A7811, Sigma-Aldrich, USA). The uptake of labeled exosomes by the cardiomyocytes was observed by using laser scanning confocal microscopy.

2.10 Echocardiography

The mice were anesthetized by intraperitoneal injection of 2,2,2-tribromoethanol (Avertin, 0.2 g/kg body weight, Sigma, St. Louis, MO, USA). The anesthetized mice were then fixed on the workbench and subjected to transthoracic echocardiography using a Vevo 2100 High-Resolution Imaging System (Visual Sonics, Canada). The left ventricular internal diameter diastolic (LVIDd) and the left ventricular internal diameter systolic (LVIDs) were measured in two-dimensional long-axis views. The left ventricular ejection fraction (EF) and fraction shortening (FS) were calculated to assess cardiac function.

2.11 Quantitative real-time polymerase chain reaction (PCR)

Total RNA was extracted from whole blood using Trizol LS solution (Invitrogen, USA). Exosomes and myocardial tissue from mice in each group were used for RNA extraction with Trizol Regent (Invitrogen, USA). Complementary DNA (cDNA) was synthesized using a reverse transcription kit (Toyobo, Japan) according to the manufacturer's instructions. Real-time quantitative polymerase chain reaction (RT-PCR) was performed using a SYBR Green PCR Master Mix (Roche, Basel, Swiss) and an Applied Biosystems 7500 Fast real time PCR system (USA) to measure the relative expression of CCRR. GAPDH or β-actin was used as an internal control for CCRR in blood samples and myocardial tissue and quantified using the 2^{-ΔΔCt} method.

The primers used in this study included: (1) CCRR forward: 5'-GT-GCTGCCATCGAAAAATCTG-3' and CCRR reverse: 5'-CTC-CCCAGACTCAATGCTTC-3'; (2) CDR1AS forward: 5'-TCTGCTCGTCTTCCAACATC-3' and CDR1AS reverse: 5'-AGAT-CAGCAGACTGGAGACG-3'; (3) ZFAS1 forward: 5'-AACCAG-GCTTTGATTGAACC-3' and ZFAS1 reverse: 5'-ATTCCATCGCCAGTTTCT-3'; (4) β -actin forward: 5'-GGCTGTATTCCCCTC-CATCG-3' and β -actin reverse: 5'-CCAGTTGGTAACAATGCCAT-GT-3'; (5) GAPDH forward: 5'-AAGAAGGTGGTGAAGCAGGC-3' and GAPDH reverse: 5'-TCCACCACCCAGTTGCTGTA-3'.

2.12 Immunofluorescence staining

Mouse hearts were fixed in 4% paraformaldehyde. For permeabilization, the slices were mounted on glass slides and incubated in PBS containing 10 mg BSA and 2% Triton X-100 for 1 hour at room temperature. After blocking with 5% BSA for 1 hour at room temperature, the slices were incubated overnight at 4°C with primary antibodies diluted in PBS: CD63 (1 : 100, ab217345, Abcam, USA) and Anti- α -actinin (1 : 200, A7811, Sigma-Aldrich, USA). Following primary antibody incubation, the samples were washed three times with PBS. Then, fluorescein-488 and fluorescein-594 secondary antibodies (1 : 200 each, Molecular Probes, Eugene, OR, USA) were added and incubated for 1 hour at room temperature in a humidified chamber. After washing three times with PBS, the samples were stained with 4',6-diamidino-2-phenylindole (DAPI) for 5 min at room temperature. Immunofluorescence images were captured and analyzed under a laser confocal microscope.

2.13 Western blot

Protein concentrations were measured with the Bicinchoninic Acid (BCA) Protein Assay Kit (Beyotime, China). Equal volumes of protein samples were separated by sodium dodecylsulfate-polyacrylamide gel electrophoresis (SDS-PAGE) and transferred to nitrocellulose (NC) membranes. The membranes were blocked with 5% non-fat milk for 1 hour at room temperature, and then incubated overnight at 4°C with primary antibodies specific for CD63 (1 : 500 dilution, Abcam, USA) and CD81 (1 : 200 dilution, Cell Signaling Technology, USA). The following day, after washing twice using PBS, the membranes were incubated with a secondary antibody (1 : 10000) for 1 hour at room temperature. Odyssey software was used to analyze the grey density of the protein bands.

2.14 Statistical analyses

Categorical data are presented as count and percentile. Continuous variables are described using means, standard error of the mean (SEM), minimum, maximum, median, and interquartile range. All statistical analyses were performed using Graph Prism

9.0. except for the ROC analysis, which was conducted with Medcalc software, and the NTA analysis, which was carried out using Origin 8.5. Student's t-test or one-way ANOVA was used to assess differences between groups, with a *P* value < 0.05 considered statistically significant.

3 Results

3.1 Basic clinical characteristics of patients in this study

We collected whole blood samples from 68 patients with AMI and 69 non-AMI control subjects to detect the expression level of CCRR. The average ischemic time of patients with AMI was within 24 h, ranging from 30 min to 24 h. Blood samples were collected at the time of infarction, with an average of 7.34 ± 0.94 h post-onset for AMI patients. The AMI group included 43 males and 25 females, while the non-AMI control group consisted of 33 males and 36 females. The mean age of AMI patients was 60.60 ± 1.30 years, comparable to the non-AMI control subjects, who had a mean age of 61.57 ± 1.08 years. There were no differences between AMI patients and non-AMI control subjects regarding age (*P* = 0.5671), hypertension (*P* = 0.1936), diabetes (*P* = 0.9034), HDL levels (*P* = 0.3831), and TG levels (*P* = 0.4304) between AMI patients and non-AMI control subjects. However, AMI patients exhibited significantly higher levels of CK-MB (*P* = 0.0011), AST (*P* = 0.0011), HBDH (*P* = 0.0425), and cTn (*P* = 0.0218) compared to non-AMI control subjects (Table 1).

3.2 Increased expression of CCRR in whole blood of patients with AMI

In our previous study, we found that CCRR regulates cardiac conduction function and has a high degree of homology between humans and mice. Moreover, we determined that CCRR is predominantly located in the cytoplasm and nucleus, where it may regulate cardiac function under pathophysiological conditions. It does so by blocking the intracellular transport of Cx43, preventing the degradation of Cx43 by binding to CIP85, and thereby improving cardiac conduction^[23]. In this study, we observed that the expression level was significantly increased in the whole blood of patients with AMI. Specifically, the circulating level of CCRR was 1.929 ± 0.1323 in AMI patients, significantly higher than the 1.000 ± 0.0544 observed in non-AMI subjects (*P* < 0.001). This represents a 92.90% increase circulating CCRR levels in AMI patients compared to non-AMI subjects (Fig.1A, Table 2). These findings suggest that CCRR is involved in the pathogenesis of MI.

Our previous study also reported significant changes in the levels of lncRNA ZFAS1 and CDR1AS in the whole blood of patients with AMI^[14]. In this investigation, ZFAS1 and CDR1AS were used

Table 1 Basic characteristic indicators and diagnostic indicators of non-AMI control subjects and myocardial infarction patients

Characteristics	Statistical items	Non-AMI control	AMI	P value
Age	N (Missing)	68 (1)	68	0.5671
	Mean (SEM)	61.57 (1.08)	60.60 (1.30)	
	Min, Max	40.00, 80.00	42.00, 82.00	
	Median	61.50	60.50	
	Range	56.00-68.00	52.00-69.00	
Gender	Male	33 (47.83%)	43 (63.24%)	0.0705
	Female	36 (52.17%)	25 (36.76%)	
	Total (Missing)	69	68	
Hypertension	Yes	35 (55.56%)	30 (44.12%)	0.1936
	No	28 (44.44%)	38 (55.88%)	
	Total (Missing)	63 (6)	68	
Smoking	Yes	20 (31.75%)	30 (44.12%)	0.1475
	No	43 (68.25%)	38 (55.88%)	
	Total (Missing)	63 (6)	68	
Diabetes	Yes	17 (26.98%)	19 (27.94%)	0.9034
	No	46 (73.02%)	49 (72.06%)	
	Total (Missing)	63 (6)	68	
HDL	N (Missing)	62 (7)	67 (1)	0.3831
	Mean (SEM)	1.1050 (0.0336)	1.7870 (0.7482)	
	Min, Max	0.530, 1.820	0.540, 51.120	
	Median	1.095	1.040	
	Range	0.9075-1.2550	0.860-1.230	
LDL	N (Missing)	62 (7)	67 (1)	0.0252
	Mean (SEM)	2.700 (0.1125)	3.059 (0.1115)	
	Min, Max	1.160, 4.870	1.520, 6.420	
	Median	2.580	2.860	
	Range	2.155-3.225	2.390-3.570	
CHOL	N (Missing)	62 (7)	67 (1)	0.0158
	Mean (SEM)	4.368 (0.1483)	4.900 (0.1577)	
	Min, Max	2.340, 8.720	2.760, 10.310	
	Median	4.245	4.740	
	Range	3.540-5.135	4.030-5.620	
TG	N (Missing)	62 (7)	67 (1)	0.4304
	Mean (SEM)	1.932 (0.1736)	2.123 (0.1681)	
	Min, Max	0.490, 7.560	0.540, 6.090	
	Median	1.620	1.670	
	Range	1.058-2.205	1.030-3.000	
AST	N (Missing)	15 (54)	49 (19)	0.0011
	Mean (SEM)	26.43 (2.668)	181.7 (24.90)	
	Min, Max	17.00, 53.00	20.00, 769.00	
	Median	23.50	85.00	
	Range	19.00-28.00	41.00-287.30	
LDH	N (Missing)	6 (63)	59 (9)	0.0514
	Mean (SEM)	226.9 (52.04)	918.5 (110.1)	
	Min, Max	136.50, 484.00	148.00, 5437.0	
	Median	184.70	674.00	
	Range	170.60-263.20	391.00-1094.0	
CK-MB	N (Missing)	30 (39)	39 (29)	0.0011
	Mean (SEM)	1.042 (0.1597)	71.63 (18.15)	
	Min, Max	0.200, 4.500	0.300, 576.20	

Continued

Table 1 Continued.

Characteristics	Statistical items	Non-AMI control	AMI	P value
CK	Median	0.720	27.60	0.0436
	Range	0.630-1.300	1.900-106.30	
	N (Missing)	6 (63)	59 (9)	
	Mean (SEM)	86.30 (13.90)	1522 (220.7)	
	Min, Max	45.10, 136.90	33.00, 6779	
HBDH	Median	77.05	844.0	0.0425
	Range	60.18-121.6	178.0-2415	
	N (Missing)	5 (64)	35 (33)	
	Mean (SEM)	118.7 (7.825)	638.5 (92.56)	
	Min, Max	101.0, 139.5	134.8, 2367	
cTn	Median	111.8	438.6	0.0218
	Range	103.6-137.4	265.4-724.4	
	N (Missing)	31 (38)	48 (20)	
	Mean (SEM)	6.682 (2.566)	21341 (7306)	
	Min, Max	0.000, 70.70	2.900, 289880	
	Median	2.210	3727	
	Range	1.400, 5.100	178.2, 14289	

AST: aspartate transaminase; CHOL: total cholesterol; CK: creatine kinase; CK-MB: creatine kinase MB; HBDH: hydroxybutyrate dehydrogenase; HDL: high density cholesterol; LDH: lactic dehydrogenase; LDL: low density cholesterol; TG: triglyceride.

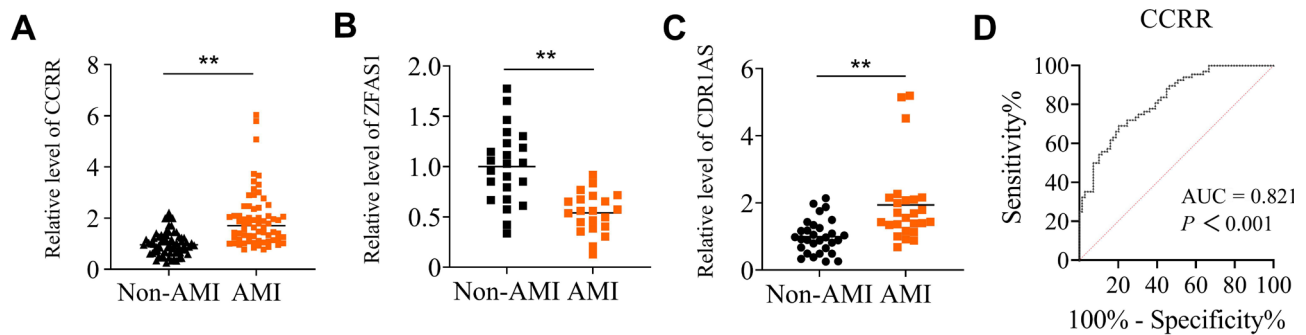


Fig. 1 Analyses of CCRR levels in whole blood of acute myocardial infarction (AMI) patients

(A) The expression levels of lncRNA CCRR in whole blood samples from AMI patients and non-AMI subjects were comparatively analyzed using qRT-PCR. $N = 68$ for AMI and $N = 69$ for non-AMI subjects. (B and C) Circulating levels of lncRNA ZFAS1 (B) and CDR1AS (C). The expression levels of lncRNA ZFAS1 in whole blood samples; $N = 21$ for AMI and $N = 23$ for non-AMI subjects. The expression levels of lncRNA CDR1AS in whole blood samples; $N = 25$ for AMI and $N = 30$ for non-AMI subjects. Data are represented as means \pm SEM; $^{**}P < 0.01$ vs. Non-AMI. (D) The area under the ROC curve (AUC) was analyzed to determine the predictive power of circulating lncRNA levels for AMI using non-AMI subjects as control.

Table 2 The Statistical Analysis of Circulating lncRNA CCRR

lncRNA	Statistical items	Non-AMI control	AMI	P value
CCRR	N (Missing)	69	68	< 0.001
	Mean (SEM)	1.0000 (0.0544)	1.9290 (0.1323)	
	Min, Max	0.257, 2.214	0.768, 6.033	
	Range	0.649, 1.247	1.146, 2.292	

as parallel controls. We found that the expression of ZFAS1 was significantly downregulated in the whole blood of AMI patients compared with the non-AMI control group, while the expression of CDR1AS was significantly up-regulated in the whole blood of AMI

patients compared to the non-AMI group (Fig.1B and C). These results, along with the findings for CCRR, demonstrate that these lncRNAs can stably exist in whole blood, are easy to detect, and provide reliable results.

3.3 The diagnostic or monitoring values of circulating CCRR for AMI

For 68 AMI patients and 69 non-AMI patients, we conducted ROC analysis to assess the diagnostic efficacy of CCRR for AMI. The AUC value for CCRR in AMI patients was 0.821 (95% CI = 0.747-0.882, Fig. 1D), with a sensitivity of 69.10% and a specificity of 79.70%, indicating that CCRR has great potential as a diagnostic marker for AMI. To assess the predictive value of lncRNA CCRR for AMI, univariate logistic regression was performed, and to exclude the impact of age, gender and blood lipid level on AMI risk, univariate logistic regression was subsequently performed in patients with AMI and in non-AMI subjects as a control group (Table 3). The univariate regression analysis of the association between lncRNA CCRR and the demographic characteristics of AMI patients and non-AMI subjects are summarized in Table 3. It is noted that the odd ratio (OR), a measure of association between circulating CCRR level and AMI, for univariate analysis was > 1 (10.31, 95% CI: 4.573-27.23, $P < 0.0001$; Table 3), which indicates that the expression level of CCRR is associated with the risk of MI. We also performed univariate regression analysis on cardiovascular disease risk factors such as patient age, sex, diabetes, HDL, LDL, TG, and CHOL. The OR values of the above factors were age (OR = 0.9899, $P = 0.5635$), gender (OR = 1.876, $P = 0.0705$), diabetes (OR = 1.049, $P = 0.9024$), HDL (OR = 1.062, $P = 0.3258$), LDL (OR = 1.581, $P = 0.0232$), TG (OR = 1.110, $P = 0.4247$), and CHOL (OR = 1.450, $P = 0.0136$). The multivariate logistic regression analysis showed that the OR values of CCRR was > 1 (12.38, 95% CI: 4.982-37.41, $P < 0.0001$) between AMI and non-AMI (Table 4). Meanwhile, we included patient age, sex, diabetes, HDL, LDL, TG, and CHOL as cardiovascular disease risk factors in the multivariate regression analysis. The results showed the following OR values for these factors: age (OR = 0.9902, $P = 0.6855$), gender (OR = 2.170, $P = 0.1338$), diabetes (OR = 1.547, $P = 0.4225$), HDL (OR = 1.020, $P = 0.8281$), LDL (OR = 1.325, $P = 0.6063$), TG (OR = 0.974, $P = 0.8951$), and CHOL (OR = 1.505, $P = 0.3319$). These data demonstrate that, after accounting for the influence of other variables, there is still a statistically significant association between CCRR and MI. The results of univariate analysis and multivariate analysis showed that CCRR could be used as independent predictors for AMI.

3.4 Change of CCRR expression in whole blood of mice with AMI

Due to the high degree of homology of CCRR between humans and mice, we investigated its expression in whole blood samples from MI model mice and sham-operated group mice at different time points of myocardial ischemia (2 h, 6 h, 12 h, 24 h). Total RNA was extracted from mouse whole blood samples and isch-

emic marginal areas of the myocardium, and real-time fluorescence quantitative PCR was performed to detect CCRR expression. As illustrated in Fig. 2, the results showed that CCRR levels in the whole blood of AMI mice increased from 0 to 24 h, compared with sham control, with the highest levels observed at 12 h. Conversely, the expression level of CCRR in the ischemic border zone tissue of MI mice decreased. These findings demonstrate that CCRR undergoes significant changes in the early stages of myocardial ischemia. Collectively, the expression of CCRR in the whole blood of AMI model mice was significantly upregulated within 24 h.

3.5 Role of exosomes in the changes of lncRNA-CCRR in whole blood and myocardium of mice with AMI

Given the high stability and detectability of lncRNA in the whole blood of both patients and mice^[24], we investigated the potential mechanisms for the increased CCRR levels in whole blood after MI, with a particular focus on exosomes. Exosomes, which carry a variety of signaling molecules including ncRNAs and proteins, play a critical role in cell-to-cell communication^[25]. Emerging evidence suggests that lncRNAs within exosomes participate in the induction of MI^[26]. We hypothesized that exosomes might act as transporters for lncRNA CCRR between the heart and the blood following AMI. To test this hypothesis, we administered GW4869 to mice *via* intraperitoneal injection to inhibit exosomes production *in vivo*^[27]. We observed an upregulation of the exosomal marker protein CD63 in the MI mice model, which was reversed by the GW4869 treatment. This indicates that exosomes production increased after AMI (Fig. 3A and B). Furthermore, colocalization of CCRR and CD63 was found in cardiomyocytes and cardiac tissues (Fig. 3C and D), indicating that CCRR is present in exosomes secreted by the myocardium. Importantly, after GW4869 injection, CCRR expression in myocardial tissue of AMI mice was significantly increased compared to AMI mice without treatment, while CCRR levels in whole blood were significantly decreased (Fig. 3E and F). These results suggest that the inhibition of exosome generation is crucial for understanding the changes in CCRR levels in myocardial tissue and whole blood following AMI.

3.6 Characterization of cardiomyocytes-derived exosomes

Exosomes were isolated from cultured cardiomyocytes under normoxic and hypoxic conditions (Fig. 4A). Transmission electron microscopy (TEM) was used to observe the morphology of exosomes derived from control and hypoxic cardiomyocytes (Fig. 4B). Nanoparticle tracking analysis (NTA) revealed that the peak diameters of normoxic and hypoxic exosomes were 78.01 nm and 79.90 nm, respectively. NTA analysis confirmed that exosomes isolated from cardiomyocytes under both conditions had similar sizes

Table 3 Univariate regression analysis for the association of CCRR with basic characteristic indicators between AMI patients and non-AMI control subject

Parameter	Estimate	SE	Wald	P value	OR	95%CI	
						lower	upper
CCRR	2.333	0.4527	26.543	< 0.0001	10.31	4.573	27.23
Age	-0.0101	0.0176	0.3327	0.5635	0.9899	0.9561	1.025
Gender	0.6293	0.3483	3.265	0.0705	1.876	0.9524	3.744
Diabetes	0.0481	0.3919	0.0150	0.9024	1.049	0.4861	2.277
HDL	0.0599	0.0957	0.3916	0.3258	1.062	0.9581	2.055
LDL	0.4579	0.2093	4.787	0.0232	1.581	1.063	2.428
TG	0.1041	0.1316	0.6266	0.4247	1.110	0.8603	1.451
CHOL	0.3719	0.1594	5.448	0.0136	1.450	1.077	2.016

HDL: high density cholesterol; LDL: low density cholesterol; TG: triglyceride; CHOL: total cholesterol.

Table 4 Multivariate regression analysis for the association of CCRR with basic characteristic indicators between AMI patients and non-AMI control subjects

Parameter	Estimate	SE	Wald	P value	OR	95%CI	
						lower	upper
CCRR	2.516	0.5112	24.22	< 0.0001	12.38	4.982	37.41
Age	-0.0099	0.0244	0.1640	0.6855	0.9902	0.9433	1.039
Gender	0.7746	0.5167	2.247	0.1338	2.170	0.8018	6.183
Diabetes	0.4361	0.5437	0.6434	0.4225	1.547	0.5370	4.609
HDL	0.01978	0.0911	0.0471	0.8281	1.020	0.9174	2.026
LDL	0.2817	0.5466	0.2656	0.6063	1.325	0.3725	3.538
TG	-0.0263	0.1997	0.0174	0.8951	0.974	0.6485	1.438
CHOL	0.4090	0.4215	0.9413	0.3319	1.505	0.7449	4.332

HDL: high density cholesterol; LDL: low density cholesterol; TG: triglyceride; CHOL: total cholesterol.

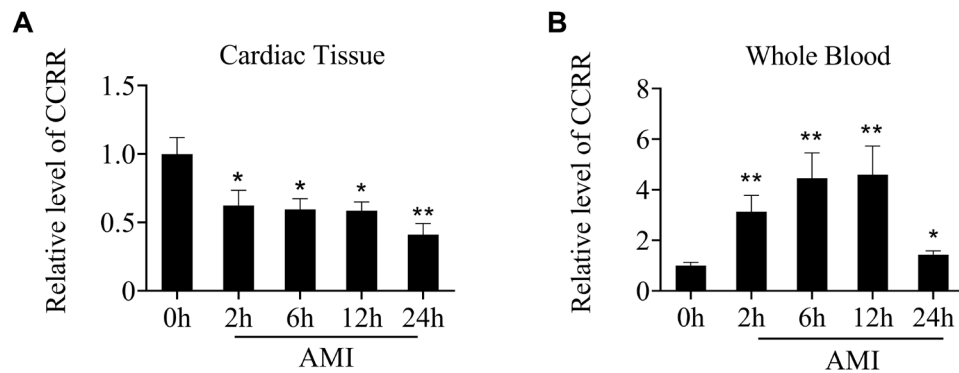


Fig. 2 The expression of lncRNA CCRR in ischemic border zone of the heart and whole blood after acute myocardial infarction (AMI) surgery at different time points (A, B) Changes of CCRR in cardiac tissues (A) and blood (B) CCRR levels in a mouse model of AMI at various time points (2 h, 6 h, 12 h and 24 h). The number of cardiac tissue sample was: $N = 20$ for sham, $N = 12$ for AMI 2 h, $N = 14$ for AMI 6 h, $N = 14$ for AMI 12 h, $N = 8$ for AMI 24 h. The number of blood sample was: $N = 27$ for sham, $N = 11$ for AMI 2 h, $N = 11$ for AMI 6 h, $N = 15$ for AMI 12 h, $N = 15$ for AMI 24 h. AMI represent acute myocardial infarction with LAD. Data are represented as means \pm SEM; * $P < 0.05$ vs. Sham, ** $P < 0.01$ vs. Sham.

ranging from 30 to 100 nm (Fig. 4C). There were no significant differences in the average size between hypoxic exosomes (Hypo-Exo) and normoxic exosomes (Nor-Exo). Western blot analysis validated the presence of exosomal biomarkers, specifically CD63 and CD81 proteins, in the isolated exosomes (Fig. 4D). To assess the uptake of exosomes by cardiomyocytes, we incubated cardiomyocytes with PKH26-labeled exosomes for 24 h and observed them under a laser scanning confocal microscope. The results

confirmed that cardiomyocytes were able to effectively uptake the PKH26-labeled exosomes (Fig. 4E).

3.7 AMI-induced cardiac injury is reduced by inhibiting exosome generation

Cardiac exosomes were isolated from both control mice and AMI mice using ultracentrifugation. Western blot analysis confirmed

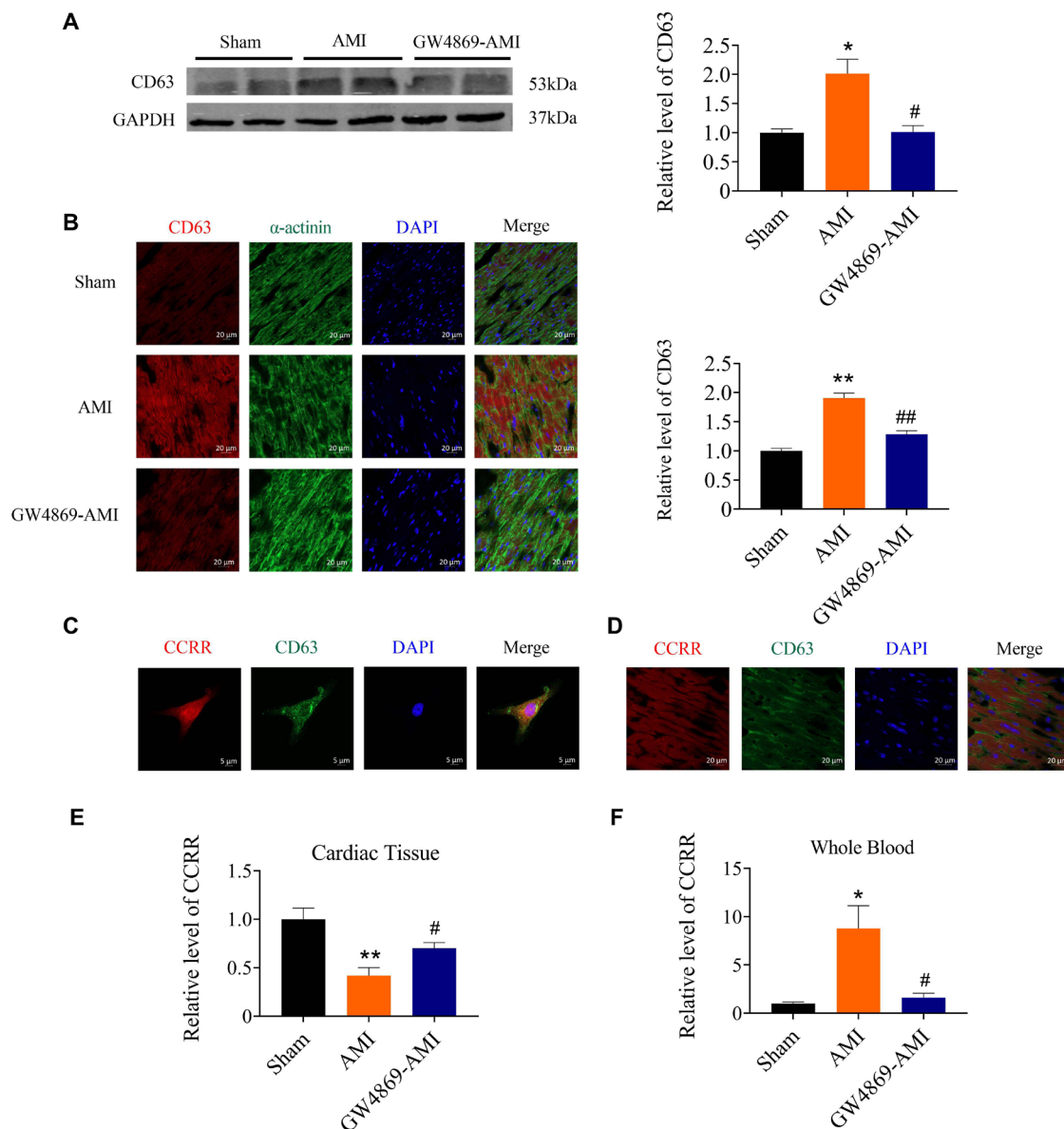


Fig. 3 Exosomes as new vesicular lipid transporters involved in changes of CCRR in whole blood after acute myocardial infarction (AMI)

(A) GW4869 inhibited CD63 expression in the heart of AMI mice. $N = 6$ per group. (B) GW4869 inhibits CD63 expression in the cytoplasm of cardiomyocytes in GW-AMI mice. CD63 was marked by red colour, α -actinin by green colour and DAPI by blue colour. Scale bar: 20 μ m. $N = 3$ per group. (C) Confocal colocalization analysis of CCRR (red) and CD63 (green) in primary cultured neonatal mouse cardiomyocytes. CCRR was marked by red colour, CD63 by green colour and DAPI by blue colour. Scale bar: 5 μ m. (D) Confocal co-localization analysis of CCRR and CD63 in mouse myocardium. CCRR was marked by red colour, CD63 by green colour and DAPI by blue colour. Scale bar: 20 μ m. (E, F) CCRR levels in myocardial tissue (E) of mice and whole blood (F) after AMI mice were treated by GW4869. $N = 16$ per group. Data are represented as means \pm SEM; * $P < 0.05$ vs. Sham, ** $P < 0.01$ vs. Sham, # $P < 0.05$ vs. AMI, ## $P < 0.01$ vs. AMI.

successful isolation of exosomes, with the detection of exosomal markers CD63 and CD81 (Fig. 5A and B). PCR analysis revealed a significant increase in CCRR levels in the cardiac exosomes of AMI mice compared to control mice. To assess the impact of inhibiting exosome generation on CCRR expression, mice were

treated with GW4869, an exosomal inhibitor, prior to undergoing AMI surgery. Results showed that while the expression levels of CD63 and CD81 in cardiac tissue were elevated following MI, they were significantly reduced after GW4869 treatment (Fig. 5B). Importantly, the CCRR levels in cardiac exosomes were also mark-

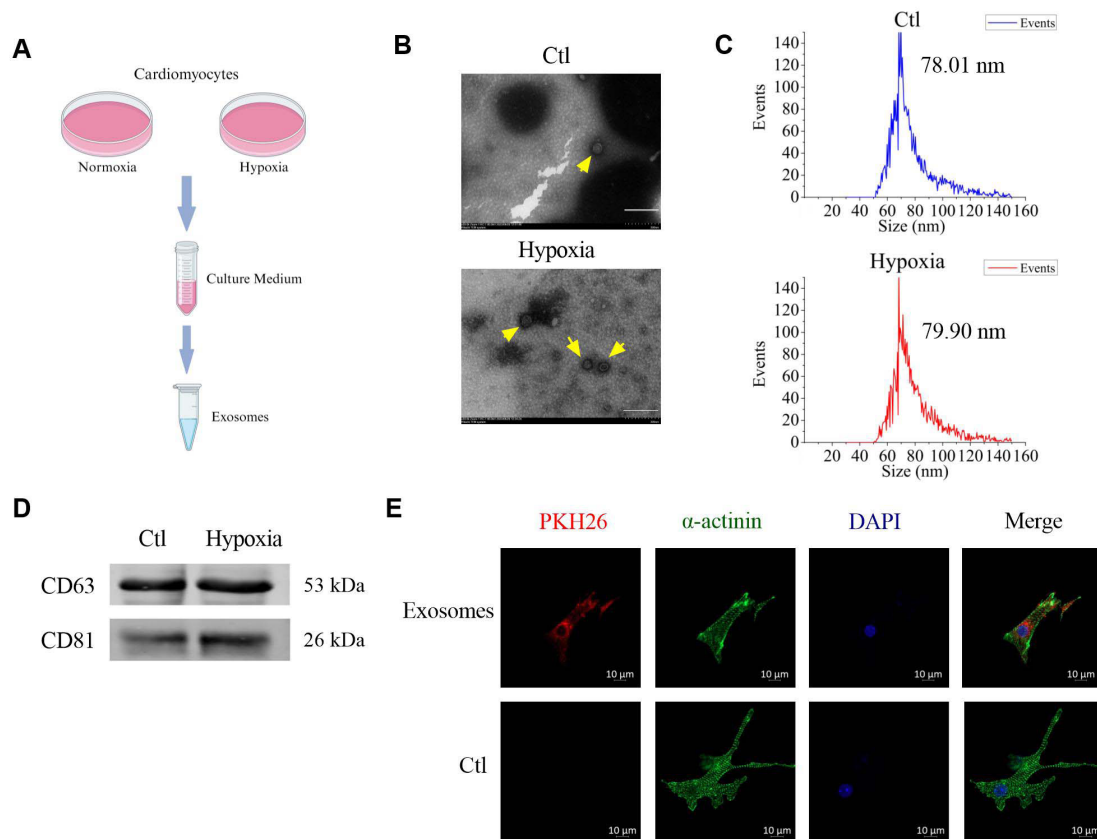


Fig. 4 Characterization of cardiomyocytes-derived exosomes

(A) Exosomes were extracted from cardiomyocyte supernatants under normoxic or hypoxic conditions. (B) Electron micrograph-analyzed cardiomyocyte exosomes. Scale bar: 200 nm. (C) The size distribution of nor-Exo and hypo-Exo determined by nanoparticle tracking analysis (NTA). (D) Western blot of exosomal marker expression in cardiomyocyte exosomes. (E) Primary neonatal mouse cardiomyocytes were cultured with PKH26-labeled exosomes or without PKH26-labeled exosomes at 37°C, 5% CO₂ for 24 h. PKH26 was marked by red colour, α -actinin by green colour and DAPI by blue colour. Scale bar: 10 μ m.

edly decreased in the GW4869-treated AMI mice (Fig. 5C). This suggests that inhibition of exosome production diminishes CCRR expression in cardiac exosomes, supporting the hypothesis that AMI releases CCRR into the circulation *via* exosomes. To investigate the therapeutic potential of cardiac exosomes on MI-induced cardiac injury, GW4869 was administered intraperitoneally to mice before MI surgery. Cardiac function was assessed 12 h post-MI using echocardiography. The results demonstrated that GW4869 significantly improved cardiac function in MI mice compared with the DMSO-treated sham control group, highlighting the potential of exosome inhibition as a strategy to mitigate AMI-induced cardiac damage (Fig. 5D-H).

3.8 Administration of CCRR-overexpressed exosomes improves cardiac function in AMI

To explore the cardioprotective effects of CCRR-overexpressed exosomes (CCRR-Exos), we injected these exosomes, derived

from the supernatant of CCRR overexpressing cardiomyocytes, into mice 12 h prior to AMI surgery (Fig. 6A). Twenty-four h post-injection, PKH26-labeled exosomes were observed in the myocardium, confirming effective uptake by cardiomyocytes (Fig. 6B). The exosomes from CCRR-overexpressing cells exhibited increased CCRR levels compared to control exosomes (NC-Exos) (Fig. 6C). Following the administration of CCRR-Exos, the CCRR expression in myocardial tissue of AMI mice was significantly elevated compared to those treated with NC-Exos (Fig. 6D). The administration of CCRR-Exos resulted in a marked improvement in cardiac function in AMI mice, as assessed by echocardiography (Fig. 6E-I). These findings suggest that CCRR-Exos exert a protective effect on cardiac function following AMI, underscoring the crucial role of CCRR in mitigating cardiac dysfunction associated with AMI.

4 Discussion

Cardiovascular disease, including ischemic heart injury, remain a

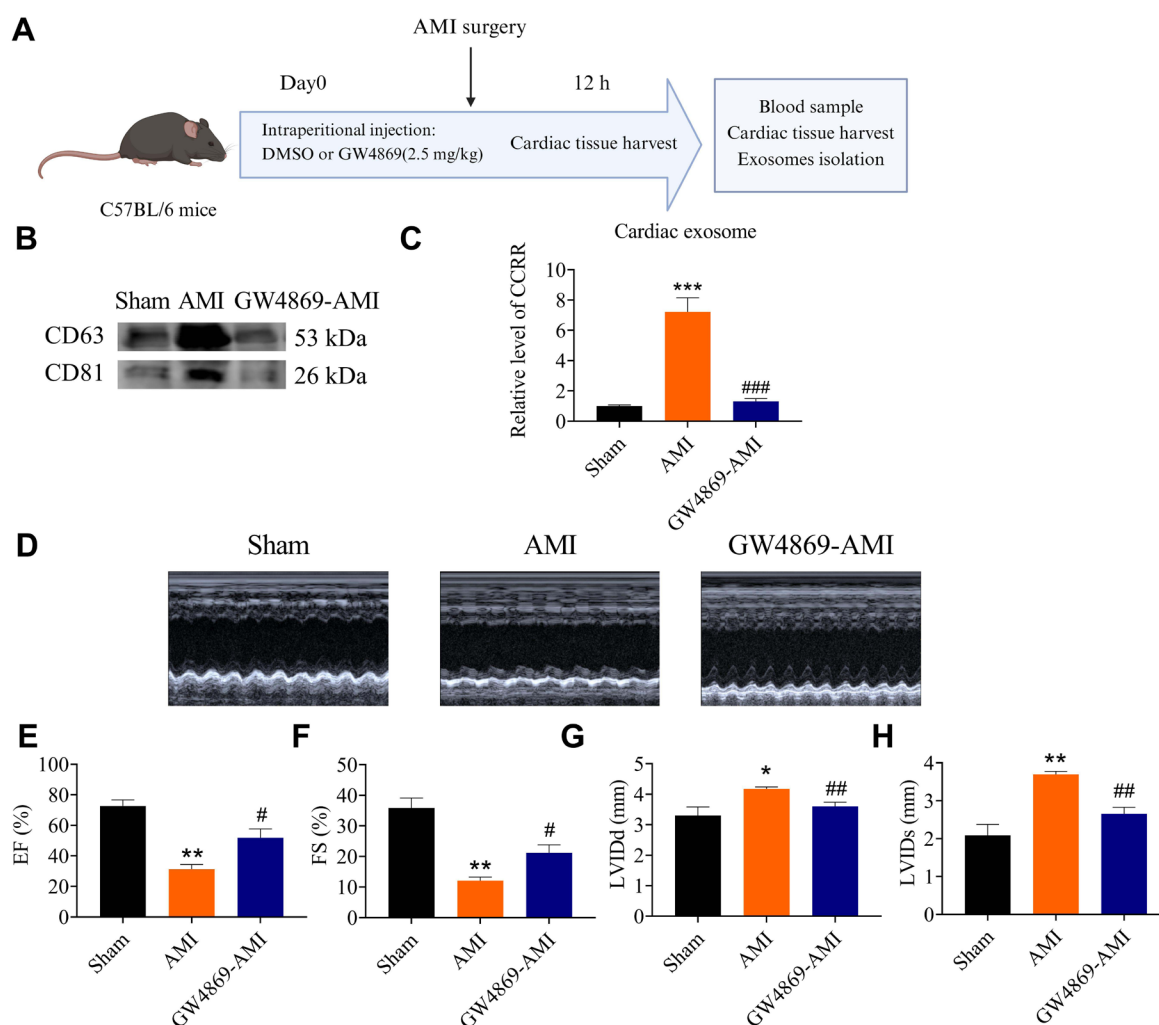


Fig. 5 GW4869 treatment mitigates myocardial infarction-induced cardiac dysfunction

(A) Flowchart of *in vivo* experimental design. (B) Western blot showing the protein level of CD63 and CD81 in Sham control mice cardiac exosomes (Sham-Exo), AMI mice cardiac exosomes (AMI-Exo) and GW4869-AMI mice cardiac exosomes $N = 3$. (C) lncRNA CCR levels in the cardiac exosomes. $N = 7$ per group. (D) Representative echocardiographic images showing heart function among the different groups in the 12 h following AMI. (E-H) Quantitative analysis of left ventricular ejection fraction (E) left ventricular fraction shortening (F) left ventricular end-diastolic diameter (G) and left ventricular systolic diameter (H) among the different groups. $N = 4$ mice per group. Data are represented as means \pm SEM; * $P < 0.05$ vs. Sham, ** $P < 0.01$ vs. Sham, *** $P < 0.001$ vs. Sham, # $P < 0.05$ vs. AMI, ## $P < 0.01$ vs. AMI, ### $P < 0.001$ vs. AMI.

leading cause of death globally^[28]. Environmental factors, such as ambient air temperature, are critical in influencing cardiovascular disease risk and mortality. Cold climates and rapid temperature changes can significantly impact cardiovascular health, with cold exposure contributing to cardiovascular diseases through several mechanisms^[29-30]. These include disruption of cardiovascular homeostasis, alterations in hemodynamics and myocardial contractility, and modulation of various molecular signaling pathways.

Given the high incidence of cardiovascular diseases in cold

regions and the limitations of traditional diagnostic methods, there is an urgent need for specific molecular biomarkers predict cardiovascular risk and injury, especially in cold climates. Personalized approaches to prevention and management of cardiovascular diseases, tailored to individual risk profiles and environmental conditions, are essential for improving patient outcomes. AMI is characterized by rapid onset, high mortality, and poor prognosis. Early diagnosis and intervention are crucial for reducing myocardial injury, complications, and improving survival and quality of life. Traditional diagnostic markers

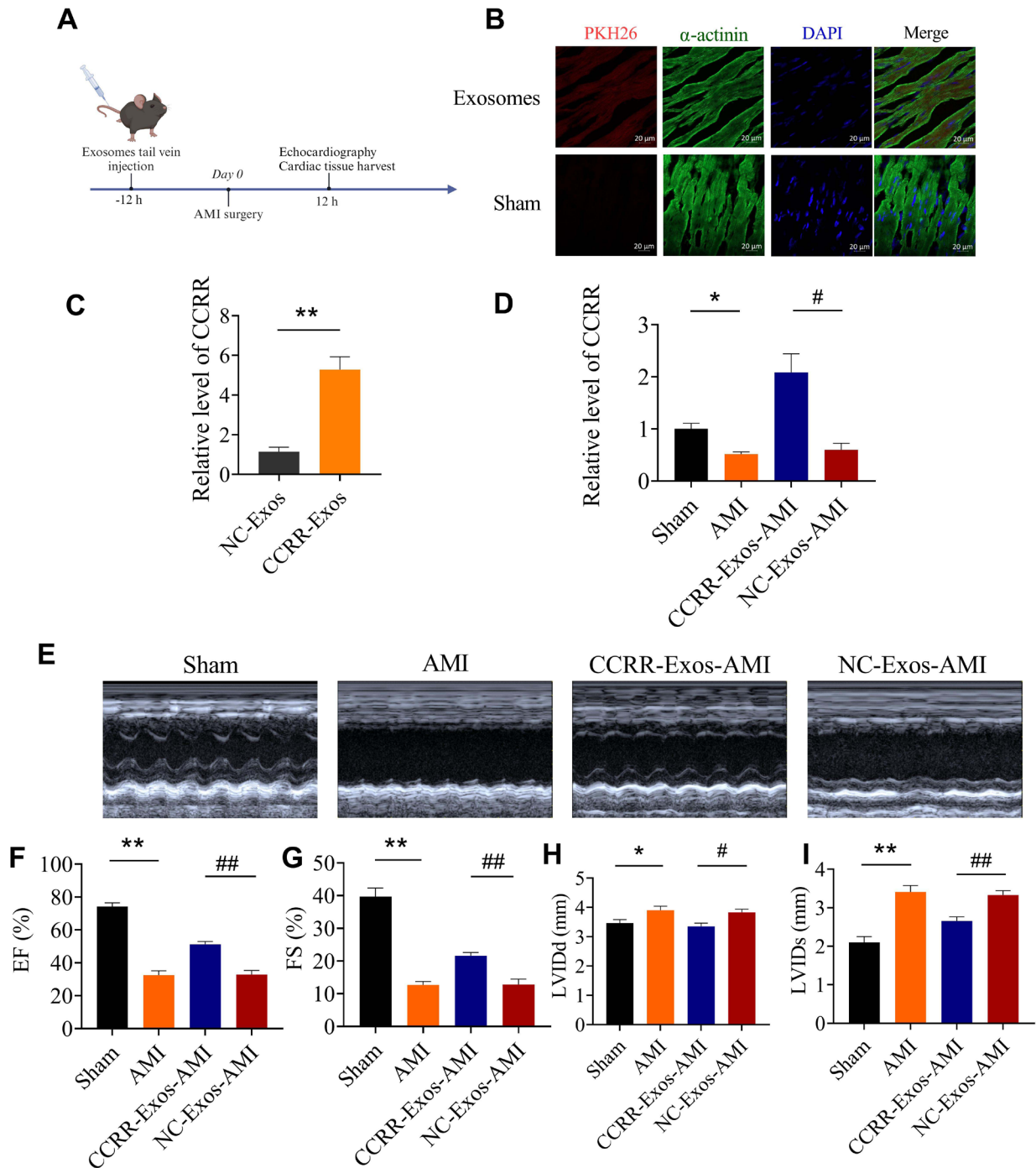


Fig. 6 Administration of CCRR overexpressed exosomes improves cardiac function in acute myocardial infarction mice

(A) Flowchart of *in vivo* experimental design. (B) Immunofluorescence images of cardiac tissue after intravenous injection of PKH26-labeled exosomes or PBS in mice. Scale bar: 20 μ m. (C) Expression level of lncRNA CCRR in exosomes. $N = 6$ per group. (D) lncRNA CCRR levels in myocardial tissue. $N = 7-8$ per group. (E) Representative echocardiographic images showing cardiac function among the different groups on the 12 h following AMI. (F-I) Quantitative analysis of left ventricular ejection fraction (F) left ventricular fraction shortening (G) left ventricular end-diastolic diameter (H) and left ventricular systolic diameter (I) among the different groups. $N = 6-8$ mice per group. Data are represented as means \pm SEM; * $P < 0.05$ vs. Sham, ** $P < 0.01$ vs. Sham, # $P < 0.05$ vs. NC-Exos-AMI; ## $P < 0.01$ vs. NC-Exos-AMI.

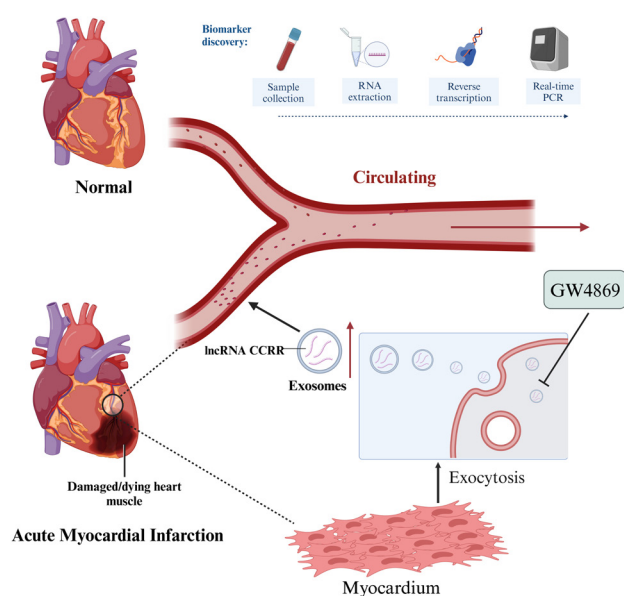


Fig. 7 Schematic illustration of delivery of the exosomal lncRNA CCRR into circulation in acute myocardial infarction injury. Exosomal lncRNA CCRR derived from hypoxic cardiomyocytes is released into circulation. Circulating exosomal lncRNA CCRR may serve as a promising novel biomarker for AMI risk prediction.

such as CK-MB, cTnI, and cTnT have been valuable for AMI diagnosis but are often limited by issues of specificity and sensitivity, influenced by factors such as age, medication, and genetics^[31-32]. lncRNAs offer promising potential as diagnostic markers for MI due to their rapid expression changes, high tissue specificity, ease of detection, and convenient sampling methods. Their use in combination with traditional biomarkers can enhance diagnostic accuracy and facilitate the development of personalized treatment strategies. This study highlights the potential of lncRNA CCRR as a diagnostic biomarker for AMI. Our findings demonstrate that CCRR levels in whole blood are significantly elevated early in the course of AMI, underscoring its role in the early detection and management of myocardial ischemia (Fig. 7).

In our previous study, we identified CCRR, which regulates cardiac conduction and exhibits high conservation. Our research demonstrated that CCRR is predominantly localized in the cytoplasm and nucleus, potentially modulating cardiac function under heart failure conditions to improve cardiac conduction^[23]. In this study, we assessed CCRR expression in the whole blood of patients with AMI within 24 h of ischemia. We found that CCRR levels were significantly increased in the blood of both AMI patients and AMI mice. The findings suggest that CCRR can be used as a diagnostic marker for AMI with high sensitivity and specificity, indicating its potential as an independent predictor and diagnostic tool for AMI.

Interestingly, CCRR may be released into the bloodstream via exosomes derived from cardiomyocytes. This aligns with the broader trend of using lncRNAs as biomarkers for MI. For example, lncRNA-UCA1, which is abundant in adult hearts, has been implicated in heart disease^[33]. Yan *et al.* reported that plasma levels of UCA1 were significantly decreased early in AMI but increased by the third day after AMI onset^[34]. Additionally, lncRNA-XIST may participate in the pathophysiological process of MI by regulating the expression of JAK2 and CDC42^[35]. To validate the reliability of potential biomarkers, we also evaluated the expression of ZFAS1 and CDR1AS as positive controls (Fig. 1B and C). Cardiomyocytes, endothelial cells, and cardiac fibroblasts can secrete exosomes, which are nanometer-sized extracellular vesicles present in the microenvironment of various cells^[36]. It has been demonstrated that exosome secretion increases under hypoxic conditions^[37-38]. Vicencio *et al.* found that plasma exosomes significantly increased under ischemic conditions^[39], and these endogenous exosomes can enhance cardiac tolerance to ischemia-reperfusion injury^[39]. Tomasoni *et al.* found that exosomes can deliver protective miRNAs that promote a microenvironment conducive to myocardial repair^[40]. These studies highlight the critical role of exosomes in the pathological development of cardiac ischemia. Following MI, cardiomyocytes release exosomes carrying CCRR into the bloodstream, resulting in decreased CCRR expression in myocardial tissue and increased CCRR levels in circulation. These results have been corroborated by both *in vivo* and *in vitro* experiments. Treatment of AMI mice with the exosome inhibitor GW4869 via intraperitoneal injection reversed the upregulation of the exosomal marker protein CD63, indicating that exosome production increased after AMI. Notably, GW4869 treatment resulted in a significant increase in CCRR expression in myocardial tissue compared with non-AMI mice, while CCRR expression in whole blood significantly decreased. This suggests that inhibiting exosome generation is crucial for altering CCRR levels in myocardial tissue and circulation following AMI. Additionally, exosomes overexpressing CCRR were found to improve cardiac function in AMI. Transmission electron microscopy was used to examine the morphology of exosomes from hypoxic cardiomyocytes, and PKH26-labeled exosomes were incubated with cardiomyocytes to observe the effects of exosome trafficking.

Collectively, our study demonstrates that circulating CCRR is a potential predictor of AMI and that its dysregulated expression represents a novel molecular mechanism underlying ischemic heart disease. CCRR holds promise as a diagnostic marker of AMI. This study, which involved analyzing blood samples from AMI patients in Northeastern China, provides a theoretical foundation for better understanding and addressing cardiovascular diseases in cold climates. However, further validation with larger clinical samples and more detailed mechanistic studies are required before CCRR can be established as a clinical diagnostic marker.

5 Limitations of the study

Our study highlights the significant role of lncRNA CCRR in diagnosing MI. However, there are notable limitations that must be addressed.

Firstly, our patients sample size is relatively small. Future research should include larger cohorts to validate these findings comprehensively. Additionally, while we focused on lncRNAs previously associated with cardiac function, this study did not explore undiscovered lncRNAs potentially related to MI onset. Nevertheless, the lncRNAs investigated in this study are closely related to heart disease and are highly expressed cardiac tissue^[41-42]. Finally, the development of lncRNA as a diagnostic marker necessitates a rigorous validation process, and standardization of lncRNA detection platform is essential for clinical application.

Author contributions

Sun L H, Xuan L N, Luo H S, Wang S and Kang K conceived and designed all experiments. Yang H and Xuan L N conducted MI mice model and functional experiments. Wang G Z, Luo H S, Zhang H L, Yang X M and Li X F performed molecular biology experiments *in vivo* and *in vitro*. Wang S J, Xuan L N, Zhang Q Q, Luo H S, Duan X M, She Y T and Liu S L performed cytology experiments. Guo J J, Chen J and Luo H S performed all the statistical analysis. Sun L H, Kang K, Xuan L N and Luo H S discussed the data and wrote this paper.

Source of funding

This work was partially supported by grants from the Natural Sci-

ence Foundation of China (81970202, 81903609), by Natural Science Foundation of Heilongjiang Province, China (LH2022H002), by the Outstanding Young Talent Research Fund of College of Pharmacy, Harbin Medical University (2019-JQ-02), 2021 (the second batch) Research Funds for affiliated research institutes in Heilongjiang Province (CZKYF2021-2-C013).

Ethical approval

All human investigators procedures were approved by the Institutional Research Board of Harbin Medical University (No. IRB5003621). All animal procedures were approved by the Institutional Animal Care and Use Committee at Harbin Medical University. All experiments complied with the guiding principles for the care and use of laboratory animals in Harbin Medical University and were approved by the Ethics Committee for Animal Experimentation of School of Pharmacy, Harbin Medical University (No. IRB5003621, No. IRB3001823).

Informed consent

For investigations of humans, written informed consent was obtained from the study participants.

Conflict of interest

The authors declare no competing interests.

Data availability statement

All data used in the study are available from the corresponding author by request.

References

- [1] Roth G A, Mensah G A, Johnson C O, *et al.* Global burden of cardiovascular diseases and risk factors, 1990-2019: update from the GBD 2019 study. *J. Am. Coll. Cardiol.*, 2020; 76: 2982-3021.
- [2] Liu S, Li Y, Zeng X, *et al.* Burden of cardiovascular diseases in China, 1990-2016: findings from the 2016 global burden of disease study. *JAMA Cardiology*, 2019; 4 (4): 342-352.
- [3] Zhao D. Epidemiological features of cardiovascular disease in Asia. *JACC: Asia*, 2021; 1 (1): 1-13.
- [4] Li X, Wu C, Lu J, *et al.* Cardiovascular risk factors in China: a nationwide population-based cohort study. *The Lancet Public Health*, 2020; 5 (12): e672-e681.
- [5] Lei J, Chen R, Yin P, *et al.* Association between cold spells and mortality risk and burden: a nationwide study in China. *Environmental Health Perspectives*, 2022; 130 (2): 027006.
- [6] Schulte C, Barwari T, Joshi A, *et al.* Noncoding RNAs versus protein biomarkers in cardiovascular disease. *Trends Mol Med*, 2020; 26: 583-596.
- [7] Emdin M, Aimo A, Vergaro G, *et al.* sST2 predicts outcome in chronic heart failure beyond NT-proBNP and high-sensitivity troponin T. *J Am Coll Cardiol*, 2018; 72: 2309-2320.
- [8] Wang Y, Sun X. The functions of lncRNA in the heart. *Diabetes Res Clin Pract*, 2020; 168: 108249.
- [9] Mozaffarian D, Benjamin E J, Go A S, *et al.* Heart disease and stroke statistics-2015 update: a report from the American Heart Association. *Circulation*, 2015; 131: e29-322.
- [10] Kopp F, Mendell J T. Functional classification and experimental dissection of long noncoding RNAs. *Cell*, 2018; 172: 393-407.
- [11] Chang G, Zhang W, Zhang M, *et al.* Clinical value of circulating

- ZFAS1 and miR-590-3p in the diagnosis and prognosis of chronic heart failure. *Cardiovasc. Toxicol*, 2021; 21: 880-888.
- [12] Sharma S, Findlay G M, Bandukwala H S, *et al*. Dephosphorylation of the nuclear factor of activated T cells (NFAT) transcription factor is regulated by an RNA protein scaffold complex. *Proc Natl Acad Sc*, 2011; 108: 11381-11386.
- [13] Viereck J, Thum T. Circulating noncoding RNAs as biomarkers of cardiovascular disease and injury. *Circ Res*, 2017; 120: 381-399.
- [14] Cao M, Luo H, Li D, *et al*. Research advances on circulating long noncoding RNAs as biomarkers of cardiovascular diseases. *Int J Cardiol*, 2022; 353: 109-117.
- [15] Zhang Y, Sun L, Xuan L, *et al*. Reciprocal changes of circulating long non-coding RNAs ZFAS1 and CDR1AS predict acute myocardial infarction. *Sci Rep*, 2016; 6: 2384.
- [16] Wang X, Wang L, Ma Z, *et al*. Early expressed circulating long noncoding RNA CHAST is associated with cardiac contractile function in patients with acute myocardial infarction. *Int J Cardiol*, 2020; 302: 15-20.
- [17] Tang Y, Zheng J, Sun Y, *et al*. MicroRNA-1 regulates cardiomyocyte apoptosis by targeting Bcl-2. *Int Heart J*, 2009; 50: 377-387.
- [18] Gao L, Liu Y, Guo S, *et al*. Circulating long noncoding RNA HOTAIR is an essential mediator of acute myocardial infarction. *Cell. Physiol. Biochem*, 2017; 44: 1497-1508.
- [19] Azat M, Huojiahemaiti X, Gao R, *et al*. Long noncoding RNA MIAT: a potential role in the diagnosis and mediation of acute myocardial infarction. *Mol Med Rep*, 2019; 20: 5216-5222.
- [20] Wang L, Wang L, Wang Q. Constitutive activation of the NEAT1/miR-22-3p/Ltb4r1 signaling pathway in mice with myocardial injury following acute myocardial infarction. *Aging (Albany NY)*, 2021; 13: 15307-15319.
- [21] Li M, Wang Y F, Yang X C, *et al*. Circulating long noncoding RNA LIPCAR acts as a novel biomarker in patients with ST-segment elevation myocardial infarction. *Med Sci Monit*, 2018; 24: 5064-5070.
- [22] Yan L, Zhang Y, Zhang W, *et al*. lncRNA-NRF is a potential biomarker of heart failure after acute myocardial infarction. *J Cardiovasc Transl Res*, 2020; 13: 1008-1015.
- [23] Zhang Y, Sun L, Xuan L, *et al*. Long non-coding RNA CCRN controls cardiac conduction *via* regulating intercellular coupling. *Nat Commun*, 2018; 9: 4176.
- [24] Khodayi M, Khalaj-Kondori M, Hoseinpour F M A, *et al*. Plasma lncRNA profiling identified BC200 and NEAT1 lncRNAs as potential blood-based biomarkers for late-onset Alzheimer's disease. *EXCLI J*, 2022; 21: 772-785.
- [25] Isaac R, Reis F C G, Ying W, *et al*. Exosomes as mediators of intercellular crosstalk in metabolism. *Cell Metab*, 2021; 33: 1744-1762.
- [26] Zheng M L, Liu X Y, Han R J, *et al*. Circulating exosomal long non-coding RNAs in patients with acute myocardial infarction. *J Cell Mol Med*, 2020; 24: 9388-9396.
- [27] Catalano M, O'Driscoll L. Inhibiting extracellular vesicles formation and release: a review of EV inhibitors. *J Extracell Vesicles*, 2020; 9, 1703244.
- [28] Crea F. How epidemiology can improve the understanding of cardiovascular disease: from mechanisms to treatment. *Eur Heart J*, 2021; 42: 4503-4507.
- [29] Lerman B, Lerman L O. "Nothing burns like the cold": Cardiovascular disease in frigid zones. *Frigid Zone Medicine*, 2022; 2 (3): 129-131.
- [30] Jin H. Increased risk of cardiovascular disease in cold temperatures. *Frigid Zone Medicine*, 2022; 2 (3): 138-139.
- [31] Oitabén A, Fonseca P, Villanueva M J, *et al*. Emerging blood-based biomarkers for predicting immunotherapy response in NSCLC. *Cancers (Basel)*, 2022; 14 (11), 2626.
- [32] Chaitman B R, Cyr D D, Alexander K P, *et al*. Cardiovascular and renal implications of myocardial infarction in the ISCHEMIA-CKD trial. *Circ Cardiovasc Interv*, 2022; 15: e012103.
- [33] Wang F, Li X, Xie X, *et al*. UCA1, a non-protein-coding RNA up-regulated in bladder carcinoma and embryo, influencing cell growth and promoting invasion. *FEBS Lett*, 2008; 582: 1919-1927.
- [34] Yan Y, Zhang B, Liu N, *et al*. Circulating long noncoding RNA UCA1 as a novel biomarker of acute myocardial infarction. *Biomed Res Int*, 2016; 2016: 8079372.
- [35] Zheng P F, Chen L Z, Liu P, *et al*. A novel lncRNA-miRNA-mRNA triple network identifies lncRNA XIST as a biomarker for acute myocardial infarction. *Aging (Albany NY)*, 2022; 14: 4085-4106.
- [36] Wang Y, Zhao R, Liu W, *et al*. Exosomal circHIPK3 released from hypoxia-pretreated cardiomyocytes regulates oxidative damage in cardiac microvascular endothelial cells *via* the miR-29a/IGF-1 pathway. *Oxid Med Cell Longev*, 2019; 2019: 7954657.
- [37] Gupta S, Knowlton A A. HSP60 trafficking in adult cardiac myocytes: role of the exosomal pathway. *Am J Physiol Heart Circ Physiol*, 2007; 292: H3052-3056.
- [38] King H W, Michael M Z, Gleadle J M. Hypoxic enhancement of exosome release by breast cancer cells. *BMC Cancer*, 2021; 12: 421.
- [39] Vicencio J M, Yellon D M, Sivaraman V, *et al*. Plasma exosomes protect the myocardium from ischemia-reperfusion injury. *J Am Coll Cardiol*, 2015; 65 (15): 1525-1536.
- [40] Tomasoni S, Longaretti L, Rota C, *et al*. Transfer of growth factor receptor mRNA *via* exosomes unravels the regenerative effect of mesenchymal stem cells. *Stem Cells Dev*, 2013; 22 (5):772-778.
- [41] Jiao L, Li M, Shao Y, *et al*. lncRNA-ZFAS1 induces mitochondria-mediated apoptosis by causing cytosolic Ca²⁺ overload in myocardial infarction mice model. *Cell Death Dis*, 2019; 10:942.
- [42] Shao Y, Li M, Yu Q, *et al*. CircRNA CDR1as promotes cardiomyocyte apoptosis through activating hippo signaling pathway in diabetic cardiomyopathy. *Eur J Pharmacol*, 2022; 922: 174915.